Biogeosciences, 6, 375–390, 2009
www.biogeosciences.net/6/375/2009/

Biogeosciences

The role of ocean transport in the uptake of anthropogenic CO_2

L. Cao[1], M. Eby[2], A. Ridgwell[3], K. Caldeira[1], D. Archer[4], A. Ishida[5], F. Joos[6], K. Matsumoto[7], U. Mikolajewicz[8], A. Mouchet[9], J. C. Orr[10], G.-K. Plattner[6,14], R. Schlitzer[11], K. Tokos[7], I. Totterdell[12,15], T. Tschumi[6], Y. Yamanaka[13], and A. Yool[12]

[1]Department of Global Ecology, Carnegie Institution, Stanford, California, USA
[2]School of Earth and Ocean Sciences, University of Victoria, Victoria, British Columbia, Canada
[3]School of Geographical Sciences, University of Bristol, Bristol, UK
[4]Department of the Geophysical Sciences, University of Chicago, Chicago, IL, USA
[5]Frontier Research Center for Global Change, Japan Agency for Marine-Earth Science and Technology, Yokohama, Japan
[6]Climate and Environmental Physics, Physics Institute and Oeschger Centre for Climate Change Research, University of Bern, Bern, Switzerland
[7]Department of Geology and Geophysics, University of Minnesota, Minneapolis, USA
[8]Max Planck Institute for Meteorology, Bundesstrasse 53, 20146 Hamburg, Germany
[9]Department of Astrophysics, Geophysics and Oceanography, University of Liege, Liege, Belgium
[10]Marine Environment Laboratories, International Atomic Energy Agency, Monaco
[11]Alfred Wegener Institute, Bremerhaven, Germany
[12]National Oceanography Centre, Southampton, UK
[13]Graduate School of Environmental Earth Science, Hokkaido University, Sapporo, Japan
[14]Institute of Biogeochemistry and Pollutant Dynamics, ETH Zürich, Universitätstr., Zürich, Switzerland
[15]Met Office Hadley Centre, Exeter, UK

Received: 2 October 2008 – Published in Biogeosciences Discuss.: 27 November 2008
Revised: 3 March 2009 – Accepted: 3 March 2009 – Published: 16 March 2009

Abstract. We compare modeled oceanic carbon uptake in response to pulse CO_2 emissions using a suite of global ocean models and Earth system models. In response to a CO_2 pulse emission of 590 Pg C (corresponding to an instantaneous doubling of atmospheric CO_2 from 278 to 556 ppm), the fraction of CO_2 emitted that is absorbed by the ocean is: 37±8%, 56±10%, and 81±4% (model mean $\pm 2\sigma$) in year 30, 100, and 1000 after the emission pulse, respectively. Modeled oceanic uptake of pulse CO_2 on timescales from decades to about a century is strongly correlated with simulated present-day uptake of chlorofluorocarbons (CFCs) and CO_2 across all models, while the amount of pulse CO_2 absorbed by the ocean from a century to a millennium is strongly correlated with modeled radiocarbon in the deep Southern and Pacific Ocean. However, restricting the analysis to models that are capable of reproducing observations within uncertainty, the correlation is generally much weaker. The rates of surface-to-deep ocean transport are determined for individual models from the instantaneous doubling CO_2 simulations, and they are used to calculate oceanic CO_2 uptake in response to pulse CO_2 emissions of different sizes pulses of 1000 and 5000 Pg C. These results are compared with simulated oceanic uptake of CO_2 by a number of models simulations with the coupling of climate-ocean carbon cycle and without it. This comparison demonstrates that the impact of different ocean transport rates across models on oceanic uptake of anthropogenic CO_2 is of similar magnitude as that of climate-carbon cycle feedbacks in a single model, emphasizing the important role of ocean transport in the uptake of anthropogenic CO_2.

Correspondence to: L. Cao
(longcao@stanford.edu)

1 Introduction

Atmospheric CO_2 is expected to increase in the near future due to continued emissions from fossil fuel burning and land use changes. A major uncertainty in projecting future climate change is how much this emitted CO_2 will remain

Published by Copernicus Publications on behalf of the European Geosciences Union.

in the atmosphere. Different processes acting on different timescales are responsible for the removal of excess CO_2 from the atmosphere. For example, the present ocean is, and the terrestrial biosphere appears to be, a net sink for anthropogenic carbon (Denman et al., 2007). Over the coming decades to centuries, the ocean is expected to continue acting as a CO_2 sink while the land could change from a net carbon sink to source (e.g., Cox et al., 2000; Bala et al., 2005). On timescales of a millennium and beyond, the reaction of dissolved CO_2 with calcium carbonate ($CaCO_3$) in deep ocean sediments will start to play an important role in buffering the human carbon perturbation (Broecker and Takahashi, 1978; Archer, 1997). On timescales of several hundred thousands of years, the still airborne anthropogenic CO_2 will be removed from the atmosphere by the weathering of silicate rocks (Walker and Kasting, 1992; Zeebe and Caldeira, 2008).

Among the processes that are responsible for the removal of CO_2 from the atmosphere, the ocean uptake plays an important role. On timescales from decades to centuries, the amount of anthropogenic CO_2 absorbed by the ocean, together with that absorbed by the terrestrial biosphere, determines CO_2 concentrations in the atmosphere. On millennial timescale, anthropogenic CO_2 remaining in the atmosphere, which has great implications for future sea level rise and ice sheet extent (Archer, 2005), will be primarily determined by the ocean uptake. In addition to regulating atmospheric CO_2, oceanic uptake of anthropogenic CO_2 modifies ocean chemistry through a process known as ocean acidification (Caldeira and Wickett, 2003; Orr et al., 2005; Cao et al., 2007; Cao and Caldeira, 2008; Steinacher et al., 2008), which threatens a variety of marine ecosystems (Royal Society, 2005)

Global carbon cycle models are used to project the uptake of anthropogenic CO_2 by the ocean and terrestrial biosphere. However, projections appear to differ widely between models on different timescales. For instance, simulated carbon uptake in the 1990s by ocean models participating in phase-II of the Ocean Carbon Model Intercomparison Project (OCMIP-2) varies between 1.98 and 3.04 Pg C (1 Pg C=10^{15} g carbon) when atmospheric CO_2 was prescribed according to the IPCC S650 CO_2 stabilization scenario (Orr et al., 2002). Accumulated oceanic carbon uptake at the time of doubling CO_2 varies by a factor of two across eleven 3-D coupled carbon cycle/climate models participating in the Coupled Climate-Carbon Cycle Intercomparison Project (C4MIP) and forced with IPCC SRES A2 emission scenario (Friedlingstein et al., 2006). The fraction of CO_2 absorbed by the ocean ranges from 24 to 34% in year 2100 and 49 to 62% in year 3000 for eight Earth system models forced by a scenario in which total CO_2 emission reaches about 1600 Pg C by year 2100 with zero emissions assumed thereafter (Plattner et al., 2008). Regarding the long-term fate of anthropogenic CO_2, model-projected airborne fraction of anthropogenic CO_2 ranges from 35 to 58% and 23 to 47% 1000 and 5000 years from now in response to a CO_2 emission pulse of about 5000 Pg C (Archer, 2005; Lenton and Britton, 2006; Ridgwell and Hargreaves, 2007; Montenegro et al., 2007). Moreover, a recent model intercomparison study shows that in response to a CO_2 emission pulse of 5000 Pg C, model-projected airborne CO_2 ranges between 20 and 30% 10 000 years after the emission pulse (Archer et al., 2009).

The discrepancy in projected atmospheric CO_2 and/or anthropogenic CO_2 uptake by the ocean across models can be attributed to modeled differences in various processes, including the rate of ocean transport, biological uptake by the ocean and terrestrial biosphere, sedimentation of calcium carbonate, and their interactions with climate change. Among these processes, ocean transport is a key player. First, the rate of ocean ventilation determines the rate by which anthropogenic CO_2 is transferred from the surface to the deep ocean. Second, on timescales over a millennium, the rate of ocean transport determines the rate by which anthropogenic CO_2 reaches ocean sediments, and carbonate ions released from dissolving $CaCO_3$ returns to the surface and further neutralize fossil fuel CO_2. Thus, ocean transport could also affect the timescale of "$CaCO_3$ neutralization" (e.g., Archer et al., 1997; Ridgwell and Hargreaves, 2007). Third, ocean transport affects biological CO_2 uptake by controlling the availability of nutrients at ocean surface and the export of organic matter from surface waters to the deep ocean. Therefore, it is important to assess how modeled ocean ventilation differs from each other and how these differences affect modeled CO_2 uptake.

The main purpose of this study is to evaluate simulated oceanic CO_2 uptake by a number of models against their simulations of geochemical tracers, and to assess the role of ocean transport in anthropogenic CO_2 uptake. Several studies have addressed some related issues. For example, Orr et al. (2001) compared the simulation of present-day anthropogenic CO_2 and bomb radiocarbon in four ocean models participating in the first phase of OCMIP. Matsumoto et al. (2004) assessed the performance of fourteen ocean models participating in OCMIP-2 in simulating radiocarbon and CFC11. Joos et al. (1999) investigated the effect of ocean transport on CO_2 uptake by conducting sensitivity simulations on vertical diffusivity in a single model. This study is built upon these previous works, but differs from them in several important aspects. First, it includes a number of prominent ocean models and Earth system models developed since OCMIP-2. These models are currently used for a variety of studies on the global carbon cycle and climate change, but their performances in simulating oceanic uptake of anthropogenic CO_2 and geochemical tracers have not been assessed in a systematic way. Second, we use the simulation of geochemical tracers to assess model-simulated anthropogenic CO_2 on timescales up to a millennium. Previous studies limited the use of geochemical tracers to assess present-day CO_2 uptake. Third, in addition to using geochemical tracers as a means to evaluate modeled ocean ventilation,here we directly

deduce the ventilation rate of each model, which provides an unambiguous way to assess the effect of ocean transport on CO_2 uptake

This paper is organized as follows. The models used in this study and simulation protocols are introduced in the next section. Model responses to different CO_2 emission pulses are presented in Sect. 3. We first investigate modeled ocean responses to a pulse release of 2 times pre-industrial CO_2, and discuss how they are related to simulated inventories of chemical tracers such as radiocarbon and Chlorofluorocarbons (CFCs). We then present surface ocean response functions that characterize the rate of ocean transport for individual models, and use them to determine CO_2 uptake in response to emission pulses of 1000 and 5000 Pg C. The impact of ocean transport on oceanic CO_2 uptake is compared to that of climate-carbon cycle feedbacks. Discussion and conclusions follow in Sect. 4.

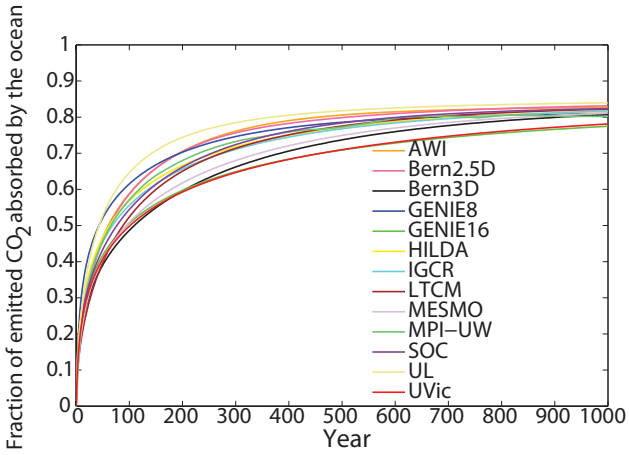

Fig. 1. Model-simulated oceanic uptake of CO_2 in response to a CO_2 pulse emission of 590.2 Pg C (corresponding to an instantaneous doubling of atmospheric CO_2 from 278 to 556 ppm).

2 Models and simulation protocols

A suite of climate/carbon-cycle models of different complexities are used in this study. These include three models derived from the Grid ENabled Integrated Earth system model (GENIE-1, Edwards and Marsh, 2005): GENIE-8 (8 ocean vertical levels, Ridgwell et al., 2007a); GENIE-16 (16 ocean vertical levels, Singarayer et al., 2008); and MESMO (16 ocean vertical levels, Matsumoto et al., 2008) (in addition to vertical resolution, these three versions of GENIE-1 differ in other aspects, see Table S1 http://www.biogeosciences.net/6/375/2009/bg-6-375-2009-supplement.pdf), the University of Victoria Earth System Climate Model (UVic, Weaver et al., 2001), Bern3D ocean model (Müller et al., 2006) with its physical core modified from Edwards et al. (1998) and Edwards and Marsh (2005), MPI-UW Earth system model (Mikolajewicz et al., 2007), high-latitude exchange/interior diffusion-advection (HILDA) model (Siegenthaler and Joos, 1992), and a modified HILDA model, LTCM (stands for the Long-term Carbon Cycle Model). In addition, archived results from five ocean carbon cycle models (AWI, Bern2.5D (previously known as PIUB), IGCR, SOC, UL) participating in OCMIP-2 and performing CO_2 pulse emission simulations (http://www.ipsl.jussieu.fr/OCMIP/) are investigated. The ocean component of these models are all coarse-resolution, non-eddy-resolving models, but they differ considerably in their configurations including the grid resolution, sub-grid scale mixing parameterizations, and surface forcing. The main characteristics of each model are listed in Table 1, and details of these models are given in Appendix A.

Carbon uptake simulations in response to an instantaneous CO_2 emission pulse were performed following the OCMIP-2 protocol (http://www.ipsl.jussieu.fr/OCMIP/phase2/simulations/Abiotic/HOWTO-Abiotic.html). Starting from the model pre-industrial state a CO_2 emission pulse of 590.2 Pg C (corresponding to an instantaneously doubling of atmospheric CO_2 concentration from 278 to 556 ppm by applying the conversion factor of 1 ppm=2.123 Pg C as used in OCMIP) is added to each model, and then the evolution of atmospheric CO_2 is determined by air-sea exchange and its transport into the ocean interior. The entire integration lasted for 1000 years. To enable direct comparison with OCMIP-2 ocean-only model simulations, only the processes relevant to ocean absorption and transport of CO_2 are included in the pulse emission simulations. Other processes, such as CO_2 uptake by the terrestrial biosphere, interaction with $CaCO_3$ sediment, climate change feedbacks (such as increased sea surface temperature, enhanced ocean stratification, and weakening of meridional overturning), and effects of CO_2-induced acidification on the biological pump (such as reduced calcification and carbonate export) are disabled. To evaluate modeled oceanic uptake of CO_2 against their skills in simulating chemical tracers, simulations of natural radiocarbon (in terms of $\Delta^{14}C$) and historical uptake of anthropogenic CO_2 and CFCs were also performed.

3 Results

3.1 Double CO_2 simulations

Time series of modeled oceanic uptake in response to an instantaneous CO_2 emission of 590 Pg C are shown in Fig. 1 (also see Table 2). Among the models shown here, UL has the largest oceanic uptake, while UVic and GENIE-16 have the lowest. The fraction of the total CO_2 emission absorbed by the ocean varies from 34 to 45%, 50 to 65%, and 77 to 84%, with a cross model mean (± 1 standard deviation, 1σ) of $37\pm4\%$, $56\pm5\%$, and $81\pm2\%$ in year 30, 100, and 1000 after the emission pulse, respectively. By the end of the 1000-year simulation the deep ocean has not yet fully equilibrated

Table 1. Key features of models used in this study.

	Horizontal resolution (Lon × Lat)	Vertical levels	Top layer thickness (m)	Surface forcing	Seasonality	Lateral mixing	Vertical diffusivity ($cm^{-2}\ s^{-1}$)[c]	Mixed layer scheme	Sea ice
AWI	5°×4° to 2.5°×2°	26	61	adjusted	No	ISOP	0.1	–	no
Bern2.5D[a]	10°–15°×basin average	14	50	EMBM	No	HOR	0.4	–	yes
Bern3D	10°×3.2° to 19.2°	32	38.9	flux, restoring	yes	ISOP, GM	0.1	–	no
GENIE-8	10°×3.2° to 19.2°	8	174.8	EMBM	No	ISOP,GM	0.27	–	yes
GENIE-16	10°×3.2° to 19.2°	16	80.8	EMBM	yes	ISOP,GM	0.25	–	yes
HILDA	high and low latitude boxes	69	75	EMBM	No	–	0.15–2.4	–	no
IGCR[b]	4°×4°	66	50	restoring	No	HOR	0.3	–	no
LTCM	high and low latitude boxes	37	75	EMBM	No	–	1.3–9.7	–	no
MESMO	10°×3.2° to 19.2°	16	45	EMBM	yes	ISOP, GM	0.1–1.2	–	yes
MPI-UW	5.6°×5.6°	22	50	AGCM	yes	ISOP, GM	[d]0.1-V_{max}	–	yes
SOC	2.5°×3.75°	20	10	flux, restoring	yes	ISOP, GM	0.1–1.5	KT	no
UL	3°×3°	20	10	bulk formula	yes	HOR	0.1–1.1	TKE	yes
UVic	3.6°×1.8°	19	50	EMBM	yes	ISOP, GM	0.3–1.3	–	yes

Abbreviations are as follows: EMBM: Energy and moisture Balance Model; HOR: Horizontal mixing parameterization; ISOP: Isopycnal mixing parameterization; GM: Gent and McWilliams (1990) mixing parameterization; KT: Kraus and Turner (1967) parameterization; TKE: Turbulent Kinetic Energy closure; AGCM: atmosphere general circulation model.
[a] Previously known as PIUB. [b] It is now recognized as FRCGC (Frontier Research Center for Global Change). [c] Vertical diffusivity decreases with depth in HILDA, while increases with depth for other models with a depth-dependent profile. [d] A single maximum vertical diffusivity for MPI-UW (V_{max}) is not available, which depends on wind speed and stratification.
Key references for each model are: AWI, Schiltzer (2002); IGCR, Yamanaka and Tajika (1996); Bern2.5D, Stocker et al. (1992); Bern-3D, Müller et al. (2006); SOC, Gordon et al. (2000); UL, Goosse and Fichefet (1999); UVic, Weaver et al. (2001); GENIE-8: Ridgwell et al., 2007a GENIE-16, Singarayer et al. (2008); MESMO, Matsumoto et al. (2008); MPI-UW, Mikolajewicz et al. (2007); HILDA, Siegenthaler and Joos (1992).

with atmospheric CO_2 in these models (even in the absence of long time-scale processes involving $CaCO_3$ in deep-sea sediments). For example, the fraction of oceanic uptake of excess CO_2 by Bern3D and LTCM is 80.7% and 82.2% in year 1000, which increases to 82.6% and 83.3% when the model ocean reaches equilibrium with perturbations in atmospheric CO_2.

Many factors could contribute to the difference in oceanic uptake of CO_2 across models, such as parameterization schemes of ocean mixing and surface boundary forcing (see Table 1). An extensive exploration of the specific role for each factor is beyond the scope of this study. Nonetheless, sensitivity simulations using GENIE-16 show that differences in the intensity of vertical mixing, model vertical resolutions, and representation of the seasonal cycle are all important in accounting for the discrepancies in modeled oceanic CO_2 uptake (Fig. S1 http://www.biogeosciences.net/6/375/2009/bg-6-375-2009-supplement.pdf). One caveat is that the OCMIP model results presented here were from abiotic runs, while other model simulations include a component of marine biology with the representation of both hard and soft tissue pumps. However, as long as the strength of biological carbon transport remains unchanged, as in the double CO_2 simulations where no feedbacks from changes in climate and biology are included, marine biology plays a minor role in the uptake of anthropogenic CO_2. This is illustrated by our sensitivity simulations (Fig. S2 http://www.biogeosciences.net/6/375/2009/bg-6-375-2009-supplement.pdf) and was also found by previous studies (Maier-Reimer, 1993; Murnane et al., 1999).

Across all models considered, positive correlations are observed between modeled CO_2 uptake and the uptake/inventories of different tracers that characterize the rate of ocean transport on different timescales (Figs. 2, 3, 4). On the decadal timescale, modeled oceanic uptake of CO_2 is strongly correlated with present-day uptake of both CFC11 and anthropogenic CO_2. Beyond a century, the correlation with the uptake of CFC11 becomes weaker, while the strong correlation with the uptake of anthropogenic CO_2 (with r greater than 0.7) extends to a few centuries. These observations are consistent with the fact that the uptake of anthropogenic CO_2 during the past is characterized by an ocean ventilation timescale of a few centuries, while the uptake of CFCs is characterized by an ocean ventilation timescale of several decades. On timescales from a century to a millennium, the amount of CO_2 absorbed by the ocean is strongly correlated with the content of natural radiocarbon in the deep ocean, which is governed by ocean ventilation over hundreds to thousands of years. This correlation is particularly strong with radiocarbon in the deep Southern (with r greater than 0.8) and Pacific Ocean (with r greater than 0.7), indicating that the processes controlling ventilation rate of the deep

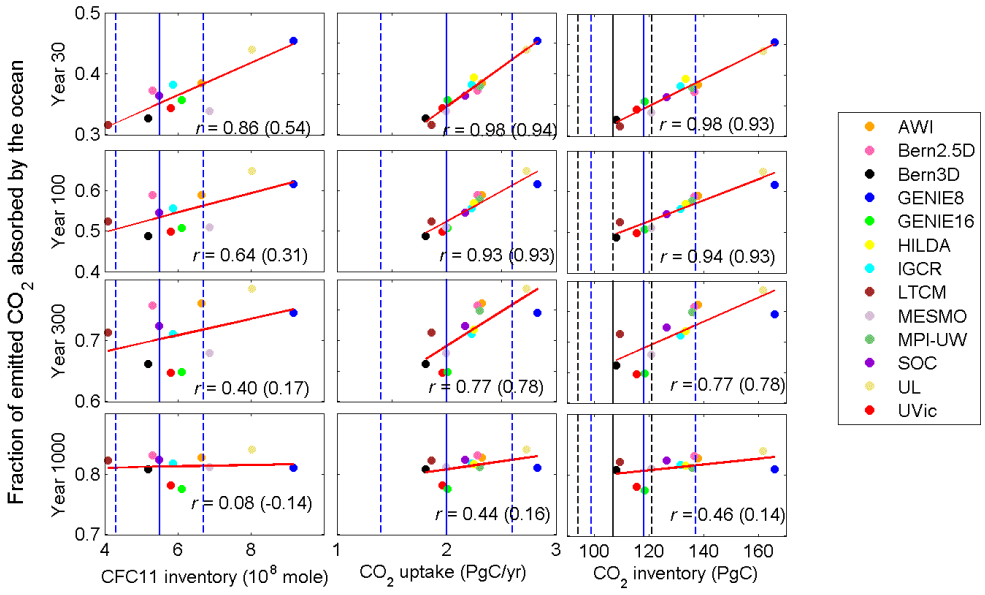

Fig. 2. Model-simulated oceanic uptake of CO_2 in response to an emission pulse of 590.2 Pg C plotted against their simulated CFC11 inventories (10^8 mole) in year 1994, mean anthropogenic CO_2 uptake (Pg C/yr) between year 1980 and 1999, and anthropogenic CO_2 inventories (Pg C) between year 1800 and 1994 (A 3% downward correction is applied to the 1990s CO_2 results for AWI, Bern2.5D, IGCR, PIUB, SOC, and UL (Orr et al., 2002), which are from simulations using the IPCC S650 scenario with 1990s atmospheric CO_2 concentrations slightly higher than the observed). The results are shown for years 30, 100, 300, and 1000 (following logarithmic distributions) after emission pulse. Vertical lines in each panel represent observational data (solid lines) and associated uncertainties (dashed lines). Observed CFC11 inventory is from Willey et al. (2004), CO_2 uptake is from Denman et al. (2007), and CO_2 inventory is from Sabine et al. (2004) (blue lines) and Waugh et al. (2006) (black lines). Also shown in each panel is the trend line and correlation coefficient r. Two correlation coefficients are shown for each panel: one with the regression taken for all models (the numbers outside the brackets) and the other with the regression taken only for models whose tracer simulation fall within the range of observational estimates (the numbers inside the brackets). Model results shown here did not include climate feedbacks. If climate feedbacks are included, uptake and inventories are slightly lower. Simulations of CFCs were not performed by MPI-UW and HILDA.

Southern and Pacific Ocean have a strong control on the long-term efficiency of the ocean to take up anthropogenic CO_2.

However, the correlation between simulated CO_2 uptake and modeled inventories of natural radiocarbon and CFC11 becomes much weaker if the regression is only applied to the models whose simulations of CFC11 and radiocarbon are within the observational bounds (Figs. 2, 3). This indicates that the inventories of global CFCs and radiocarbon of a few selected water masses, as shown here, do not provide a stringent constraint on modeled CO_2 uptake. Nevertheless, they can still be used as a first-order constraint on model's performance in simulating CO_2 uptake. For example, if model-simulated natural radiocarbon is used as an indicator for their projections of oceanic CO_2 uptake, OCMIP models presented here and GENIE-8 would appear to overestimate the amount of CO_2 taken up by the ocean on timescales from a few centuries to a millennium.

When the data-based tracer inventories are used as metrics to assess model's performance in simulating ocean dynamics, improved skills in simulating ocean transport are seen in most of the recently developed models since the ocean carbon cycle modeling efforts of OCMIP-2. This is especially true for the simulation of natural radiocarbon (Fig. 3, Table 2). One exception is GENIE-8 (Ridgwell et al., 2007a) which has a more highly ventilated ocean than the other models and for this reason overestimates the inventories of both radiocarbon and CFC11. However, use of this model has been generally restricted to long time-scale (>1000 yr) processes, particularly involving deep-sea sediment interaction with the ocean and weathering and in which it performs comparably to the higher vertical resolution version ("GENIE-16") (Archer et al., 2009).

3.2 Surface ocean response functions

Arguably, over timescales less than a millennium, the most important factor in the oceanic uptake of anthropogenic CO_2 is the rate of surface-to-deep ocean transport. However, other factors, such as the rate of air-sea exchange and buffering capacity of the carbonate system owing to the differences in modeled total carbon, alkalinity, temperature, and salinity (Table 3) will obscure the role of ocean transport in CO_2 uptake. To separate the effect of ocean transport from other factors, we adopt the method of Joos et al. (1996) to determine

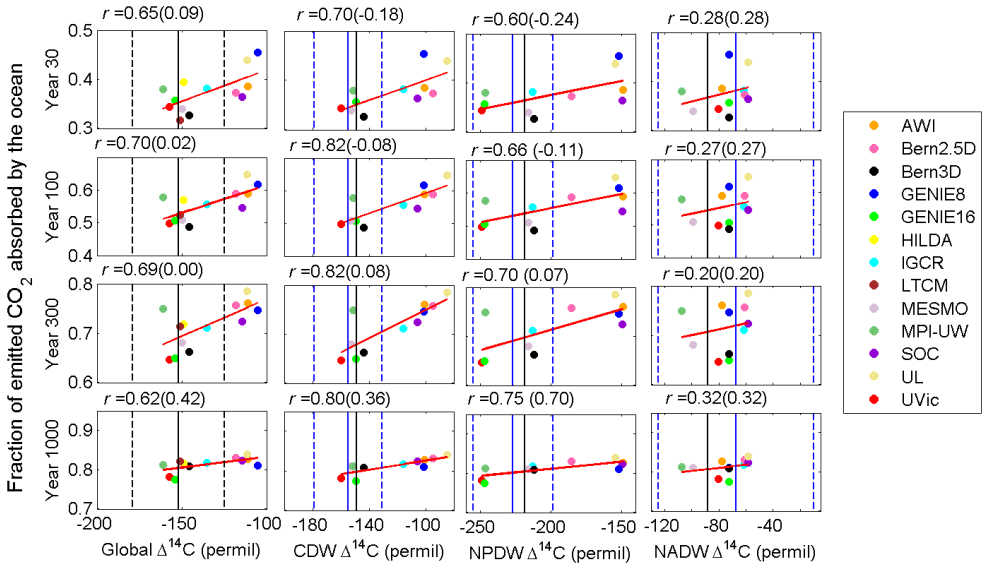

Fig. 3. Model-simulated oceanic uptake of CO_2 in response to an emission pulse of 590.2 Pg C plotted against their simulated natural radiocarbon (permil) of the global ocean, Circumpolar Deep Water (CDW, 90–45° S, 1500–5000 m), North Pacific Deep Water (NPDW, Equator-60° N, 1500–5000 m), and North Atlantic Deep Water (NADW, Equator-60° N, 1000–3500 m). The results are shown for years 30, 100, 300, and 1000 (following logarithmic distributions) after emission pulse. Vertical lines in each panel represent observational data (solid lines) from Global Data Analysis Project (GLODAP) (Key et al., 2004) and associated uncertainties (two standard deviation, dashed lines). Analysis of Matsumoto et al. (2004) using the GLODAP bottle data is represented by blue lines, and our analysis using regridded GLODAP data are represented by black lines. Also shown in each panel is the trend line and correlation coefficient r. Two correlation coefficients are shown for each panel: one with the regression taken for all models (the numbers outside the brackets) and the other with the regression taken only for models whose radiocarbon simulation fall within the range of observational estimates (the numbers inside the brackets).

Table 2. Model-simulated oceanic uptake of CO_2 in response to an emission pulse of 590.2 Pg C and simulation of geochemical tracers. Bold numbers are those within the range of observational estimates.

	Fraction of CO_2 absorbed by the ocean in response to CO_2 doubling (%)				Natural $\Delta^{14}C$				Historical uptake		
	Yr 30	Yr 100	Yr 300	Yr 1000	Global	NADW	NPDW	CDW	CO_2 uptake (Pg C/yr)	CO_2 inventory (Pg C)	CFC (10^8 mole)
AWI	38.5	58.9	76.1	82.7	−111.0	**−77.8**	−149.0	−100.9	**2.32**	**137.8**	**6.65**
Bern2.5D	37.3	58.8	75.7	83.1	−118.3	**−61.0**	−185.3	−95.0	**2.28**	**136.5**	**5.30**
Bern3D	32.7	48.7	66.2	80.8	**−145.5**	**−72.2**	**−212.0**	**−143.8**	**1.81**	**108.0**	**5.19**
GENIE-8	45.4	61.6	74.6	81.0	−105.2	**−72.6**	−151.8	−101.4	2.83	165.8	9.16
GENIE-16	35.7	50.7	64.9	77.5	**−153.9**	**−72.3**	**−246.9**	**−149.3**	**2.01**	**118.3**	**6.10**
HILDA	39.5	56.9	71.8	81.6	**−149.0**				**2.25**	**133.2**	
IGCR	38.2	55.7	71.1	81.7	**−135.2**	**−61.3**	**−212.9**	−115.6	**2.23**	**131.4**	**5.87**
LTCM	31.6	52.4	71.3	82.2	**−151.0**				**1.86**	**109.2**	4.08
MESMO	33.9	51.0	68.0	81.1	**−150.0**	**−99.0**	**−216.0**	**−153.0**	**2.00**	**120.8**	6.87
MPI-UW	38.0	57.7	74.8	81.2	**−161.2**	**−107.6**	**−246.2**	**−151.2**	**2.30**	**135.7**	
SOC	36.4	54.5	72.4	82.4	−114.3	**−58.5**	−149.1	−105.8	**2.17**	**126.5**	**5.48**
UL	43.9	64.8	78.5	84.0	−111.3	**−58.3**	−154.4	−85.0	2.73	161.5	8.03
UVic	34.4	49.8	64.7	78.1	**−157.5**	**−80.3**	**−248.7**	**−159.6**	**1.96**	**115.4**	**5.80**
Observation[a]					−151±27.0	−67.3±57.4	−222.6±28.2	−155.0±24	2.0±0.6	118±19	5.5±1.2

[a] The values of natural $\Delta^{14}C$ are taken from Matsumoto et al. (2004) assuming an uncertainty of $\pm 2\sigma$. Observed CFC11 inventory is from Willey et al. (2004), CO_2 uptake is from Denman et al. (2007), and CO_2 inventory is from Sabine et al. (2004).

surface ocean pulse response functions that characterize the rate of surface-to-deep ocean transport. The theoretical justification of the ocean pulse response functions is that the dynamics of a linear system can be fully characterized by its pulse (or Green's) function, and the transport of tracers in the ocean is described by a set of linear equations under steady state (constant circulation). Both atmospheric and surface ocean pulse response functions have therefore been used to

Table 3. Modeled global mean surface ocean fields at steady state.

	Air-sea exchange rate (mole m^{-2} year-^{1}ppm^{-1})	Alkalinity (μmol/kg)	DIC (μmol/kg)	Temperature (°C)	Salinity
AWI	0.061	2310.0	1999.3	16.1	35.0
Bern2.5D	0.061	2310.0	1984.0	18.9	34.8
Bern3D	0.057	2260.3	1950.2	18.1	34.6
GENIE-8	0.058	2304.5	1989.4	18.5	35.0
GENIE-16	0.057	2271.5	1954.7	19.2	34.9
HILDA	0.054	2300.0	2003.9	18.2	35.0
IGCR	0.061	2310.0	1985.0	19.7	34.8
LTCM	0.061	2285.2	1983.3	16.5	34.6
SOC	0.061	2310.0	1936.6	19.8	34.6
UL	0.061	2310.0	1994.2	18.8	34.7
UVic	0.060	2296.9	1985.0	17.8	34.7

compare the uptake characteristics of anthropogenic carbon by ocean transport models (Maier-Reimer and Hasselmann, 1987; Sarmiento et al., 1992; Joos et al., 1996) and to build cost-efficient substitutes of more complex models for the uptake of carbon, heat and other tracers (Joos and Bruno, 1996). As a way to represent the rate of surface-to-deep ocean transport, the use of surface ocean pulse response functions overcomes the problem arising from nonlinearity of the carbon chemistry and gives more accurate results compared to atmospheric pulse response functions.

The use of surface ocean response functions is based on the reasoning that surface concentration of dissolved inorganic carbon (DIC_s) at a certain time t can be represented by the convolution integral of earlier carbon input, i.e. the air-sea carbon flux (f) at time t', multiplied by the fraction of the flux that is still found in the surface layer after time $t - t'$ (ocean surface response, r_s). This can be represented by the following equation (from Eq. 2 of Joos et al., 1996)

$$DIC_s(t) = \frac{1}{h}\int_{t0}^{t} f(t')r_s(t-t')dt' + DIC_s(t_0) \qquad (1)$$

where h is model top layer thickness and t_0 is the time at which surface ocean is in equilibrium with the deep ocean. Given the complete history of surface carbon concentration (DIC_s) and air-sea carbon flux (f), the ocean surface response (r_s) can be determined from the above equation.

Using model output of annual and global mean surface DIC and air-sea flux from pulse simulations, surface ocean response functions at the yearly resolution were derived from the above equation for a subset of models (see Appendix B for a detailed description of how the response functions are solved). The results are shown in Fig. 5a. These responses represent the fraction of excess carbon added to the surface ocean that is still found in the ocean surface after a certain time, and therefore is a measure of the rate by which tracers (CO_2 here) are transported from the surface to the deep ocean. A validation of the derived surface ocean response functions is given in Appendix C.

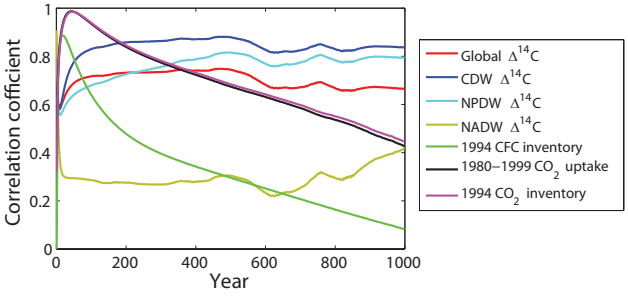

Fig. 4. Temporal evolution of correlation coefficient between model-simulated oceanic CO_2 uptake in response to an emission pulse of 590.2 Pg C and their simulated natural $\Delta^{14}C$, CFC inventory (10^8 mole), CO_2 inventory (Pg C), and CO_2 uptake (Pg C/yr) (All models results are included in the regression analysis here). On timescales from decades to a few centuries, modeled oceanic absorption of CO_2 emitted is strongly correlated with present-day uptake and inventory of anthropogenic CO_2. On timescales from a century to a millennium, the amount of CO_2 released absorbed by the ocean is strongly correlated with the content of natural radiocarbon in the deep Southern and Pacific ocean. CDW: Circumpolar Deep Water (90–45° S, 1500–5000 m); NPDW: North Pacific Deep Water (Equator-60° N, 1500–5000 m); NADW: North Atlantic Deep Water (Equator-60° N, 1000–3500 m).

It is not appropriate to compare surface ocean response functions as shown in Fig. 5a directly with each other because models have different surface layer depths (Table 1), which would lead to different response functions (Joos et al., 1996). To compare the dynamical behavior of each model directly, we normalize the derived ocean surface responses to a uniform surface ocean depth of 50 m, and the differences in the normalized ocean surface response functions represent primarily differences in the rate of surface-to-deep transport

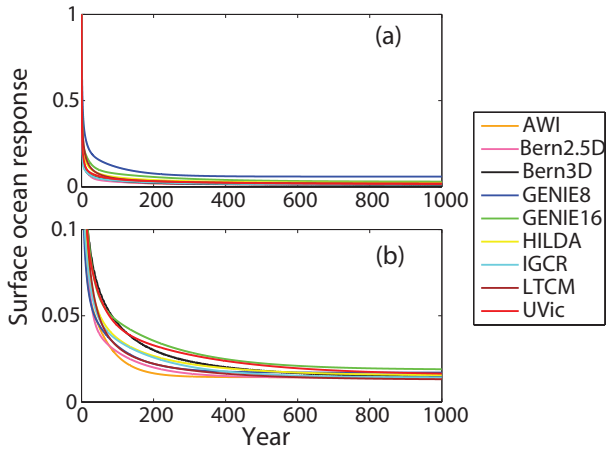

Fig. 5. Ocean surface responses which represent the fraction of an initially added amount of carbon to the surface ocean that remains in the surface after a certain time **(a)** ocean surface responses determined from the 590.2 Pg C CO_2 emission pulse simulations for individual models; **(b)** the same responses as (a), but normalized by a uniform surface depth of 50 m by multiplying each response by 50 m and divided by the top layer thickness of each model. Note that different scales are used in (a) and (b).

between models (Fig. 5b). The comparison of Fig. 5b with Fig. 1 indicates that models with faster transport from the surface to the deep ocean (lower values of ocean surface response) show greater CO_2 uptake by the ocean, suggesting that differences in the rate of ocean transport are mainly responsible for differences in simulated carbon uptake across models.

3.3 Effect of ocean transport and climate change on anthropogenic CO_2 uptake

We further investigate the effect of ocean transport on modeled oceanic CO_2 uptake using the ocean response functions derived above. The purpose of using ocean response functions are twofold: First, as discussed above, it separates the role of ocean transport from other factors such as air-sea exchange and carbonate buffering in affecting CO_2 uptake; Second, it is not practical to rerun the full OCMIP models to look at their responses to atmospheric CO_2 perturbations other than doubling CO_2. Ocean response functions provide an efficient substitute for these models. Following the method of Joos et al. (1996), we constructed a surface ocean response model to calculate oceanic CO_2 uptake in response to pulse CO_2 emissions of different sizes. Input and parameters to the model include: the normalized surface response functions (Fig. 5b) that represent the rate of surface-to-deep ocean transport for corresponding full models, a representation of surface DIC concentrations as a function of ocean surface pCO_2 derived from GENIE-16 full model runs that represent buffering capacity of the carbonate system, a surface ocean depth of 50 m, an ocean area of 3.61×10^{14} m^2, and a global mean air-sea exchange rate of 0.061 mol m^{-2} yr^{-1} ppm^{-1} taken from Broecker et al. (1986). Given these model settings, differences in simulated CO_2 uptake by the response model are caused only by different rates of ocean transport across full models. Emission scenarios considered here include CO_2 emission pulses of 1000 and 5000 Pg C. A total CO_2 pulse size of 1000 Pg C corresponds to the cumulative CO_2 emissions by the end of the century from some of the comparably modest IPCC scenarios (For example, IPCC SRES A1T scenario has a cumulative CO_2 emission of 1038 Pg C from 1990 to 2100), while the 5000 Pg C release is roughly equivalent to the amount of available conventional fossil fuel resource (IPCC, 2001).

To compare the effect of ocean transport on CO_2 uptake with that of feedbacks from interactions between climate change and the ocean carbon cycle, oceanic CO_2 uptake simulations in response to 1000 and 5000 Pg C CO_2 emission pulses were performed by a suite of climate/carbon-cycle models, including UVic, GENIE-8, GENIE-16, MESMO, HILDA, and MPI-UW used in the 590 Pg C emission pulse simulations and two additional models, CC_SED (Archer 2005) and CLIMBER-2 (Brovkin et al., 2007) (refer to Appendix A for a brief description of the CC_SED and CLIMBER-2 model). Results of pulse emission simulations from these models were also reported in a recent model intercomparison study for long-term fate of fossil fuel CO_2 (Archer et al., 2009). For each pulse emission simulation, each model was run twice: one with the coupling between climate change and the ocean carbon cycle and the other without it; the difference between these two simulations represents the effect of climate change on carbon uptake. Since our emphasis in this study is on oceanic uptake of anthropogenic CO_2, processes other than ocean uptake, including uptake by the terrestrial biosphere and deep sea $CaCO_3$ sediment, were disabled in the simulations presented here.

The rate of ocean transport affects physical uptake of anthropogenic CO_2 from the ocean surface to the deep ocean, while climate change affects the physical, chemical, and biological uptake of anthropogenic CO_2 through changes in temperature, circulation, and marine biology. As shown in Fig. 6, the effect of climate change in all models is to decrease oceanic uptake of anthropogenic CO_2 (increase atmospheric CO_2 concentrations by assuming a neutral terrestrial biosphere), but the magnitude of climate change effect varies widely between models. This discrepancy could be attributed to modeled differences in changes to temperature, circulation, and marine biology, and their interactions with the ocean carbon cycle, which merits further investigation.

It is noted that the absolute values of atmospheric CO_2 concentrations calculated from surface ocean response model runs depend on the choices of parameters used in the calculations (e.g., ocean area, air-sea exchange rate, buffering capacity of the carbonate system), but differences between model runs are much less sensitive to input parameters. What we are interested here is not the absolute values of projected

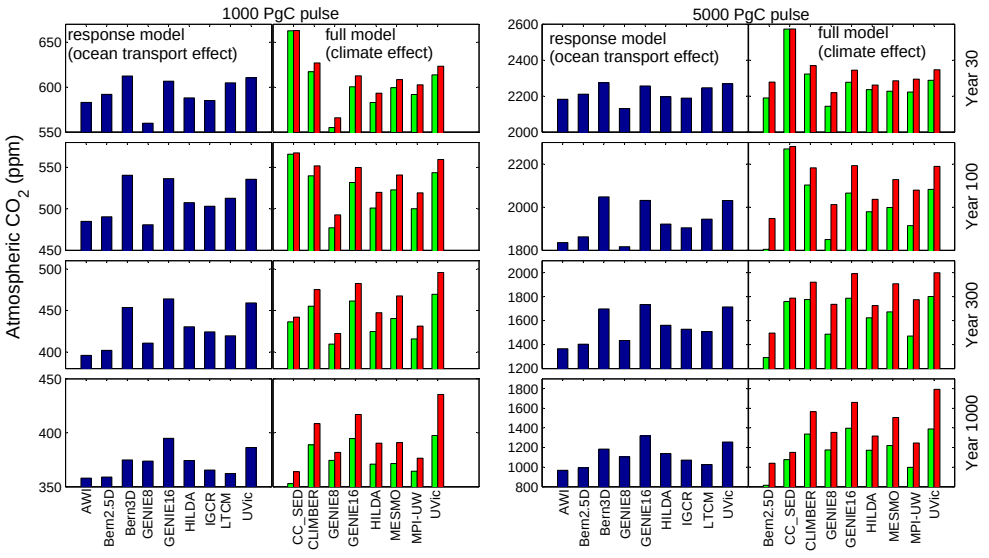

Fig. 6. Projected atmospheric CO_2 concentrations (by assuming a neutral terrestrial biosphere) in response to 1000 and 5000 Pg C emission pulses using surface ocean response model (dark blue bars) and full model runs with the inclusion of climate feedbacks on the ocean carbon cycle (red bars) and without it (green bars). The differences in CO_2 concentrations calculated by ocean response model runs are a result of differences in the rate of surface-to-deep ocean transport across models, while the differences in CO_2 concentrations calculated by full model runs are a result of climate feedbacks on the ocean carbon cycle in a single model associated with changes in temperature, circulation, and marine biology. It is shown that the effect of different steady state ocean transport rates across models on projected atmospheric CO_2 concentrations is comparable to that of climate-carbon cycle feedbacks in a single model (by assuming a neutral terrestrial biosphere).

atmospheric CO_2, but the difference in projected CO_2 concentrations as a result of different ocean transport across models, compared to that as a result of climate feedback on the ocean carbon cycle in a single model.

Figure 6 shows that the effect of different ocean transport across models on projected atmospheric CO_2 concentrations is comparable to that of climate-carbon cycle feedbacks in a single model (by assuming a neutral terrestrial biosphere). For example, 100 years after CO_2 emission pulse of 5000 Pg C the range of differences in projected CO_2 concentration caused by different ocean transport is 231 ppm, compared with a maximum difference of 165 ppm as a result of climate change feedback simulated by MPI-UW. At the same time, the spread of projected CO_2 concentrations due to differences in ocean transport across models is 88 (one standard deviation, 1σ) and 176 (2σ) ppm, compared with the difference of 108 ± 51 ppm (mean$\pm1\sigma$) associated with climate change feedbacks in a single model. 1000 years after CO_2 emission pulse of 5000 Pg C, the range of difference in projected CO_2 concentration as a result of transport difference is 351 ppm, compared with the maximum climate change effect of 404 ppm simulated by UVic. Meanwhile, the spread of projected CO_2 concentrations due to differences in ocean transport across models is 119 (1σ) and 238 (2σ) ppm, compared with the difference of 228 ± 93 (mean $\pm1\sigma$) associated with climate change feedbacks in a single model.

Presumably, models that realistically simulate inventories of geochemical tracers yield more reliable projections of CO_2 uptake. If we only consider models that realistically simulate global CFC and radiocarbon at different basins against observational estimates (Bern3D, GENIE-16, UVic), the difference in simulated CO_2 uptake between these models owing to differences in ocean transport are much smaller than that associated with climate feedbacks in a single model. This indicates that the simulations of geochemical tracers help to reduce the uncertainty in the projection of oceanic CO_2 uptake. For comparison, the uncertainty in climate effect on carbon uptake, which includes feedbacks from changes in temperature, circulation, and marine biology, is much more difficult to constrain by observations.

4 Discussion and conclusions

In the study of oceanic uptake of anthropogenic CO_2, there has been a history of investigating the effect of climate change on the ocean carbon cycle (e.g., Maier-Reimer et al., 1996; Sarmiento et al., 1998; Joos et al., 1999; Plattner et al., 2001; Chuck et al., 2005; Friedlingstein et al., 2006; Zickfeld, 2007; Plattner et al., 2008), and recently on the potential effects of ocean acidification (e.g., Heinze, 2004; Gehlen et al., 2007; Ridgwell et al., 2007b). In this study we investigate the role of ocean transport in CO_2 uptake for a suite of models, including ocean carbon cycle models participating in OCMIP and recently developed Earth system models. Using ocean response functions deduced from each model

that characterize the modeled rate of surface-to-deep-ocean transport, it is found that differences in steady state ocean ventilation rate across models can lead to discrepancies in projected oceanic CO_2 uptake that are as large as that caused by climate-carbon cycle feedbacks in a single model. This suggests that in the efforts reducing uncertainties in the projection of oceanic CO_2 uptake, careful attention should be paid to modeled ocean ventilation, while continued efforts being made to narrow down the uncertainty associated with climate-carbon cycle feedbacks.

The strong correlation between simulated CO_2 uptake and geochemical tracers across all models shows that the simulation of geochemical tracers such as CFCs and radiocarbon can be used as metrics to assess modeled CO_2 uptake by the ocean. However, for the models that reproduce observational inventories of geochemical tracers, there is no clear relationship between the modeled uptake of radiocarbon/CFCs and CO_2. Here, we only looked at a greatly reduced set of metrics (global CFC inventory, and the ^{14}C signature of a few selected water masses) and not the full 3-D fields of CFCs and radiocarbon. Thus, one may conclude that the selected set of metrics is not sufficient to fully constrain CO_2 uptake. In addition to the widely-used geochemical tracers including CFCs and radiocarbon (Maier-Reimer, 1993; Marchal et al., 1998; Orr et al., 2001; Matsumoto et al., 2004), the simulation of other biogeochemical tracers that hold complementary information about ocean dynamics is expected to better constrain and improve the models' simulation of ocean ventilation (e.g., Doney 1999; Dutay et al., 2004; Müller et al., 2006; Ito and Deutsch 2006; Najjar et al., 2007; Cao and Jain, 2008). For example, Dutay et al. (2004) evaluated the model deep-ocean circulation with the help of ^3He; Ito and Deutsch et al. (2006) evidenced that argon provides a good diagnostic of the basin-scale diapycnal diffusivity. Cao and Jain (2008) found that the modeling of phosphate helps to detect model deficiencies in the parameterization of ocean mixing that is not evident in the simulation of radiocarbon. A reliable simulation of ocean transport is not only important for the projection of CO_2 uptake, but also for the projection of heat uptake, both of which have great implication for the long-term commitment of climate change.

Appendix A

Model description

A1 OCMIP Models

A detailed description of models participating in the OCMIP-2 CO_2 pulse emission simulations (AWI, Bern2.5D, IGCR, SOC, UL) can be found in Orr et al. (2002). A brief description of each OCMIP model presented in this study is given here.

A2 AWI

The AWI model used in this study follows the approach of ocean circulation model of Schlitzer (1995). It has recently been extended to include biogeochemical nutrients and carbon cycles (Schlitzer, 2002). Unlike dynamical models that use approximations to the momentum equation and external forcing at the sea-surface to calculate the time-varying ocean circulation by applying a time-stepping procedure, the AWI model has a steady 3-D flow field representing the steady-state, annual mean circulation of the ocean.

A3 Bern2.5D

Bern2.5D (previously known as PIUB) is a physical-biogeochemical climate model that consists of a zonally averaged ocean model (Wright and Stocker, 1992; Wright and Stocker, 1998), coupled to an atmospheric energy balance model (Stocker et al., 1992). The model includes a basic representation of the carbon cycle, both marine (Marchal et al., 1998) and terrestrial (Siegenthaler and Oeschger, 1987) components. The marine biological model is based on the classical Redfield approach, and phosphate is used as a limiting nutrient for biological production.

A4 IGCR

The IGCR model was developed based on the ocean physical/biogeochemical model used in Yamanaka and Tajika (1996) for the study on the vertical fluxes of particulate organic matter and calcite. The physical variables are given by the general circulation model with the same finite differential scheme as the GFDL model.

A5 SOC

The model used by the SOC group is the ocean component of the coupled ocean-atmosphere model developed by the Hadley Centre for Climate Research and Prediction, part of the UK Meteorological Office. The version of the Hadley Centre model used for the GOSAC (Global Ocean Storage of Anthropogenic Carbon) simulations is HadCM3L, a coarse resolution form of the HadCM3 model (Gordon et al., 2000).

A6 UL

The UL model results from the CLIO (Coupled Large-scale model, Goosse, 1998) coupled with a comprehensive and prognostic ocean carbon model LOCH (Mouchet and Francois, 1996).

A7 Bern3D

The Bern3D model (Müller et al., 2006) is a cost-efficient, seasonally forced three-dimensional frictional geostrophic balance ocean model. Its physical core is based on the work by Edwards et al. (1998) and Edwards and Marsh (2005) and

has been modified to feature distinct coefficients for isopycnal diffusion and Gent-McWilliams transport parameterizations, 32 depth layers, and an implicit numerical scheme for vertical diffusion. The transport parameters have been tuned toward observed chlorofluorocarbon inventories and deep ocean radiocarbon signatures. Sea surface temperatures are constrained by restoring and sea surface salinities by flux boundary conditions. An additional anomalous uniform freshwater surface flux of 0.15 Sv from the Atlantic to the Pacific basin is applied in order to intensify and deepen the Atlantic meridional overturning circulation. Forcing fields for wind stress are derived from the NCEP data. The implementation of biogeochemical cycling in the Bern3D model closely follows the OCMIP-2 protocols. However, prognostic formulations are applied to compute the production of organic matter, $CaCO_3$, and opal shells (Parekh et al., 2008; Tschumi et al., 2008).

A8 CC_SED

CC_SED was described by Archer (2005). It uses the HAMOCC2 stationary annual mean flow to transport geochemical tracers. The temperature of the ocean is offset uniformly with a 1000-year response time, relaxing to a target temperature determined by a deep-ocean climate sensitivity of 3°C. It is coupled to a sediment model (Archer, 1996) and weathering feedbacks are also included (Berner and Kothavala, 2001).

A9 CLIMBER-2

CLIMBER-2 consists of a two-dimensional atmosphere and a two-dimensional multi-basin dynamic ocean. The climate model is coupled to a terrestrial biosphere model (VECODE) and a phosphate-limited ocean biogeochemical cycle model (Brovkin et al., 2002, 2007; Ganopolski et al., 1998).

A10 The GENIE-1 model

The three versions of the Grid ENabled Integrated Earth system model (GENIE-1) employed in this study (GENIE-8, GENIE-16, MESMO) are all based on the same fast climate model of Edwards and Marsh (2005), which features a reduced physics (frictional geostrophic) 3-D ocean circulation model coupled to a 2-D energy-moisture balance model (EMBM) of the atmosphere and a dynamic-thermodynamic sea-ice model. The ocean model includes a representation of marine carbon cycling that parameterizes biogenically induced geochemical fluxes based on a phosphate control of biological productivity, and calibrated against observational datasets of ocean geochemistry (Ridgwell et al., 2007a). The primary differences between the three versions of GENIE-1 (GENIE-8, GENIE-16, MESMO) concern the vertical resolution, means of parameter value calibration, and parameter values as described below and listed in Table S1 http://www.biogeosciences.net/6/375/2009/bg-6-375-2009-supplement.pdf.

A11 GENIE-8

"GENIE-8" divides the model ocean into 8 vertical levels and has non-seasonal climatology identical to that described in Ridgwell et al. (2007a). Parameter values controlling climate were obtained by means of an ensemble Kalman filter (EnKF) methodology described in Hargreaves et al. (2004), with annual mean climatological observations of ocean salinity and temperature together with surface air temperature and humidity assimilated.

The marine carbon cycle was also calibrated by means of EnKF as described in Ridgwell et al. (2007a), but in addition to assimilating information concerning modern observations of ocean phosphate and alkalinity distributions, experimental observations of pH impacts on plankton calcification inform the prior uncertainties for calcification rate power (η) (Ridgwell et al., 2007b).

A12 GENIE-16

"GENIE-16" employs a 16 vertical level version of the ocean circulation component, and is forced by seasonal insolation (but annual average wind stress). The climatology of this configuration of GENIE-1 has been calibrated by means of a multi-objective tuning process as described in Matsumoto et al. (2008), using exactly the same observational climatological data as for the EnKF calibration of GENIE-8 (Hargreaves et al., 2004) (except at increased vertical resolution in the ocean). Temperature diffusion around Antarctica (90–60° S) is additionally reduced by 75% in the 2-D atmospheric energy balance module to capture some of the relative (seasonal) isolation of the atmosphere in this region. The resulting configuration of the climate model and resulting climatology is identical to that described in Singarayer et al. (2008).

The biogeochemical parameters are calibrated by the same multi-objective tuning process described in Matsumoto et al. (2008) and against the same 3-D ocean phosphate and alkalinity data-sets as for GENIE-8, but without additional observational constraints on plankton calcification sensitivity (i.e., as per Ridgwell et al., 2007a). In addition, to ensure numerical stability of the calculation of atmosphere-ocean surface gas equilibrium, the time-stepping between ocean biogeochemistry and circulation is reduced to 1:2, compared to the 1:5 ratio used in GENIE-8 (Ridgwell et al., 2007a).

A13 MESMO

Derived from GENIE-1 and like GENIE-16, MESMO has 16 vertical levels and is forced by seasonal insolation. An important distinguishing feature of MESMO is the use of depth-dependent vertical diffusivity in the ocean. This improves significantly the ventilation of the interior ocean such

that the deep ocean $\Delta^{14}C$ as well as the inventories of anthropogenic carbon and CFCs are consistent with data-based estimates. In addition, biological production occurs in the top two layers above the compensation depth of 100 m and is modified by additional parameters, such as diagnosed mixed layer depth and temperature. In the steady state control run, the annual export production of POC is 10.6 Pg C and of $CaCO_3$ is 1.0 Pg C. A detailed description of the MESMO model is given in Matsumoto et al. (2008).

A14 HILDA

The High-Latitude Exchange-Interior Diffusion/Advection (HILDA) model is a box advection/diffusion model with transport parameters calibrated to match the ocean distribution of natural and bomb-produced radiocarbon (Siegenthaler and Joos, 1992). Here, the model has been applied in its mixed-layer impulse response form (Joos et al., 1996). The model, in combination with representations of the terrestrial biosphere, has been used for CO_2 projections in the IPCC Second and Third Assessment Report (Joos et al., 2001), in IPCC technical papers, and to calculate Global Warming Potentials for the Kyoto Protocol. The model includes an energy balance formulation and the equilibrium climate sensitivity has been set here to 3.2 K for a nominal CO_2 doubling.

A15 LTCM

The Long-term Carbon Cycle Model (LTCM) is a modified and extended ocean carbon cycle model based on the HILDA box advection/diffusion model of Siegenthaler and Joos (1992). The structure of the physical ocean model is built based upon the HIDAL model, but with some modifications. First, the advection of water from the deep high latitude ocean into low latitude ocean occurs at all depths instead of only at the bottom ocean as in the HILDA model. Second, unlike the original HILDA model in which vertical diffusivity decreases with ocean depth, vertical diffusivity in LTCM increases with depth following Bryan and Lewis (1979). The values of vertical diffusivity and other ocean transport parameters are calibrated against the recent data-based observations of natural radiocarbon (Key et al., 2004). The implementation of biogeochemical cycling closely follows the OCMIP-2 protocols, but biological carbon uptake is parameterized by the Michaelis-Menten type uptake kinetics instead of by restoring surface phosphate to observations as in OCMIP-2. A 1-D sediment column lies at the bottom of each ocean layer following ocean hypsometry and each column is divided into 10 vertical levels with a total depth of 10 cm. The solid component of sediment includes $CaCO_3$ and refractory materials. Dissolved inorganic carbon and alkalinity in the pore water exchange with those of ocean water through diffusion. A parameterization of carbonate and silicate weathering as a function of temperature and CO_2 concentrations are included based on the GEOCARB model of Berner and Kothavala (2001). In addition, an energy balance atmosphere is coupled to the ocean model.

A16 MPI-UW

MPI-UW (Mikolajewicz et al., 2007) consists of a coupled coarse-resolution atmospheric general circulation model ECHAM3 (Roeckner et al., 1992) and an updated version of the Large Scale Geostrophic ocean model (LSG) (Maier-Reimer et al., 1993). The ocean carbon cycle is represented by HAMOCC3 ocean biogeochemistry (Winguth et al., 1994). The land biosphere is simulated using the dynamic vegetation model LPJ (Sitch et al., 2003).

A17 UVic

The University of Victoria Earth System Climate Model (UVic 2.8) model consists of a vertically integrated, energy/moisture balance, atmospheric model with dynamic feedbacks, coupled to a modified version of the MOSES2 land surface model, the MOM2 ocean general circulation model, and a dynamic/thermodynamic sea-ice model (Weaver et al., 2001; Meissner et al., 2003). Ocean carbon is simulated by means of an OCMIP-type inorganic carbon-cycle model and a marine ecosystem model, solving prognostic equations for nutrients, phytoplankton, zooplankton, and detritus (Schmittner et al., 2008). Isopycnal mixing and flux corrected transport were used in the ocean model with diapycnal diffusion specified as a horizontally constant, Bryan-Lewis profile. The only three parameters that have been changed from the default 2.8 configuration are the ocean biology fixed production ratio of carbonate to carbon (changed from 0.02 to 0.018), the e-folding depth for carbonate remineralization (changed from 4500 m to 6500 m) and the scale height for carbon in the atmosphere (changed from 7900 m to 8049 m).

Appendix B

Solving ocean response functions

In practice we solve Eq. (B1)

$$\mathrm{DIC}_s(t_0) = \frac{1}{h}\int_{t0}^{t} f(t')r_s(t-t')dt' + \mathrm{DIC_s}\ (t_0) \qquad \text{(B1)}$$

by solving the following equation

$$\Delta\mathrm{DIC}(n) = \frac{1}{h}\sum_{1}^{n} \Delta f(i) r_s(n-i+1) \qquad \text{(B2)}$$

where $\Delta\mathrm{DIC}(n)$ is the difference in global and annual mean surface DIC concentration between the control simulation and doubling CO_2 pulse simulation at year n; $\Delta f\ (i)$ is the

Table C1. Historical CO_2 uptake (Pg C) simulated by full model runs and corresponding surface ocean response model runs. A 3% downward correction is applied to the 1990s CO_2 uptake for AWI, Bern2.5D, and IGCR (Orr et al., 2002), which are from simulations using the IPCC S650 scenario with 1990s atmospheric CO_2 concentrations slightly higher than the observed.

	1980–1999		1765–2000	
	full model	response model	full model	response model
AWI	46.4	44.7	160.0	159.0
IGCR	44.5	43.6	149.1	151.2
Bern2.5D	46.3	45.5	155.5	155.1
Bern3D	36.2	35.8	123.5	120.0
UVic	39.2	37.1	135.3	130.3
GENIE-8	56.5	56.1	187.9	184.0
GENIE-16	40.1	38.6	134.1	132.9
LTCM	37.2	37.5	121.1	122.2

difference in global and annual mean air-sea CO_2 flux between the control simulation and doubling CO_2 pulse simulation at year i, h is the top model layer thickness, and r_s $(n-i+1)$ is the ocean response function at year $n-i+1$.

Given the complete history of model output of yearly ΔDIC and Δf, ocean response function r_s at each year can be solved in sequence as follows:

$$n = 1 \quad \Delta\mathrm{DIC}(1) = \frac{1}{h}\Delta f(1) r_s(1) \tag{B3}$$

$$n = 2 \quad \Delta\mathrm{DIC}(2) = \frac{1}{h}[\Delta f(1) r_s(2) + \Delta f(2) r_s(1)] \tag{B4}$$

$$n{=}3\,\Delta\mathrm{DIC}(3){=}\frac{1}{h}[\Delta f(1) r_s(3){+}\Delta f(2) r_s(2){+}\Delta f(3) r_s(1)] \tag{B5}$$

Appendix C

Validation of surface ocean response functions

To test how well ocean response functions derived from 590 Pg C emission pulse simulations represent the rate of ocean transport for individual models, we constructed a surface ocean response model following Joos et al. (1996) to simulate historical CO_2 uptake by the ocean. Input to the surface ocean response model are: the prescribed CO_2 concentrations, the relationship between modeled surface DIC and pCO_2 derived from each model's 590 Pg C emission pulse simulation, the thickness of top model layer, the rate of air-sea gas exchange, and surface ocean response functions for each model (Fig. 5a). Oceanic CO_2 uptake simulated by full model runs and the corresponding surface ocean response model runs are compared in Table C1. Close agreement in oceanic carbon uptake is observed between full and response model calculations with the largest difference less than 5%, suggesting that surface ocean response functions essentially capture the overall strength of surface-to-deep ocean transport for the corresponding full models. The discrepancy is mainly due to the fact that the response model does not take into account natural variability of ocean transport and the spatial variability of carbon uptake.

Edited by: J. Middelburg

References

Archer, D.: A data-driven model of the global calcite lysocline, Global Biogeochem. Cy., 10, 511–26,1996.

Archer, D. Kheshgi, H., and Maier-Reimer, E.: Multiple timescales for neutralization of fossil fuel CO_2, Geophys. Res. Lett., 24(4), 405–408, 1997.

Archer, D.: Fate of fossil fuel CO_2 in geologic time, J. Geophys. Res., 110, C09S05, doi:10.1029/2004JC002625, 2005.

Archer, D., Eby, M., Brovkin, V., et al.: Atmospheric lifetime of fossil-fuel carbon dioxide, Annu. Rev. Earth Pl. Sc., in press, 2009.

Bala, G., Caldeira, K., Mirin, A., Wickett, M., and Delire, C.: Multicentury changes to the global climate and carbon cycle: Results from a coupled climate and carbon cycle model, J. Climate, 18(21), 4531–4544, 2005.

Berner, R. A. and Kothavala, Z.: GEOCARB III: A revised model of atmospheric CO_2 over phanerozoic time, Am. J. Sci, 301, 182–204, 2001.

Broecker, W. S. and Takahashi, T.: Neutralization of fossil fuel CO_2 by marine calcium carbonate, in The Fate of Fossil Fuel CO_2 in the Oceans, edited by: Andersen, N. R. and Malahoff, A., 213, Plenum Press, New York, 1978.

Broecker, W. S., Peng, T. H., Ostlund, G., and Stuiver, M.: The distribution of bomb radiocarbon in the ocean, J. Geophys. Res., 90, 6953–6970, 1985.

Broecker, W. S., Ledwell, J. R., Takahashi, T., et al.: Isotopic versus micrometeorologic ocean CO_2 fluxes, J. Geophys. Res., 91, 10517–10527, 1986.

Brovkin, V., Bendtsen, J., Claussen, M., Ganopolski, A., Kubatzki, C., and Petoukhov, V.: Carbon cycle, vegetation and climate dynamics in the Holocene: Experiments with the CLIMBER-2 model, Global Biogeochem. Cy., 16(4), 1139, doi:10.1029/2001GB001662, 2002.

Brovkin, V., Ganopolski, A., Archer, D., and Rahmstorf, S.: Lowering of glacial atmospheric CO_2 in response to changes in oceanic circulation and marine biogeochemistry, Paleoceanography , 22, PA4202, doi:10.1029/2006PA001380, 2007.

Bryan, K. and Lewis, L. J.: A water mass model of the world ocean, J. Geophys. Res., 84, 2503–2518, 1979.

Caldeira, K. and Wickett, M. E.: Anthropogenic carbon and ocean pH, Nature, 425, 365–365, 2003.

Cao, L., Caldeira, K., and Jain, A. K.: Effects of carbon dioxide and climate change on ocean acidification and carbonate mineral saturation, Geophys. Res. Lett., 34, L05607, doi:10.1029/2006GL028605, 2007.

Cao, L. and Jain, A. K.: Learning about the ocean carbon cycle from observational constraints and model simulations of multiple tracers, Clim. Change, 89, 45–66, doi:10.1007/s10584-008-9421-1, 2008.

Cao, L. and Caldeira, K.: Atmospheric CO_2 stabilization and ocean acidification, Geophys. Res. Lett., 35, L19609, doi:10.1029/2008GL035072, 2008.

Chuck, A., Tyrrell, T., Totterdell, I. J., and Holligan, P. M.: The oceanic response to carbon emissions over the next century: investigations using three ocean carbon cycle models, Tellus, 57B, 70–86, 2005.

Cox, P., Betts, R., Jones, C. D., Spall, S. A., and Totterdell, I. J.: Acceleration of global warming due to carbon-cycle feedbacks in a coupled climate model, Nature, 408, 184–187, 2000.

Denman, K. L., Brasseur, G., Chidthaisong, A., et al.: Coupling between changes in the climate system and biogeochemistry, in: Climate Change 2007: The physical science basis. Contributing of working group I to the Fourth Assessment Report of the Intergovernmental Panel on Climate Change, 2007.

Doney, S. C.: Major challenges confronting marine biogeochemical modeling, Global Biogeochem. Cy., 13, 705–714, 1999.

Doney, S. C., Lindsay, K., Caldeira, K., et al.: Evaluating global ocean carbon models: The importance of realistic physics, Global Biogeochem. Cy., 18, GB3017, doi:10.1029/2003GB002150, 2004.

Dutay, J. C., Jean-Baptistea, P., Campin, J.-M., et al.: Evaluation of OCMIP-2 ocean models' deep circulation with mantle Helium-3, J. Mar. Syst., 481(4), 15–36, doi:10.1016/j.jmarsys.2003.05.010, 2004.

Edwards, N. R. Willmott, A. J., and Killworth, P. D.: On the role of topography and wind stress on the stability of the thermohaline circulation, J. Phys. Oceanogr., 28, 756–778, 1998.

Edwards, N. R. and Marsh, R.: Uncertainties due to transport-parameter sensitivity in an efficient 3-D ocean-climate model, Clim. Dynam., 24(4), 415–433, 2005.

Friedlingstein, P., Cox, P., Betts, R., et al.: Climate-carbon cycle feedback analysis: results from the C4MIP model intercomparison, J. Climate, 19, 3337–3353, 2006.

Ganopolski, A., Rahmstorf, S., Petoukhov, V., and Claussen, M.: Simulation of modern and glacial climates with a coupled global model of intermediate complexity, Nature, 371, 323–326, 1998.

Gebbie, G., Heimbach, P., and Wunsch, C.: Strategies for nested and eddy-permitting state estimation, J. Geophys. Res., 111, C10073, doi:10.1029/2005JC003094, 2006.

Gehlen, M., Gangstø, R., Schneider, B., Bopp, L., Aumont, O., and Ethe, C.: The fate of pelagic $CaCO_3$ production in a high CO_2 ocean: a model study, Biogeosciences, 4, 505–519, 2007, http://www.biogeosciences.net/4/505/2007/.

Gent, P. R. and McWilliams, J. C.: Isopycnal mixing in ocean circulation models, J. Phys. Oceanogr., 20, 150–155, 1990.

Goosse, H.: Modelling the large-scale behavior of the coupled ocean–sea-ice system, Ph.D. thesis, Universite Catholique de Louvain, Louvain-la-Neuve, Belgium, 231 pp., 1998.

Goosse, H. and Fichefet, T.: Importance of ice-ocean interactions for the global ocean circulation: A model study, J. Geophys. Res., 104, 23337–23355, 1999.

Gordon, C., Cooper, C., Senior, C. A., Banks, H., Gregory, J. M., Johns, T. C., Mitchell, J. F. B., and Wood, R. A.: The simulation of SST, sea ice extents and ocean heat transports in a version of the Hadley Centre coupled model without flux adjustments, Clim. Dynam., 16, 147–168, 2000.

Hargreaves, J. C., Annan, J. D., Edwards, N. R., and Marsh, R.: An efficient climate forecasting method using an intermediate complexity Earth System Model and the ensemble Kalman filter, Clim. Dynam., 23(7–8), 745–760, 2004.

Heinze, C.: Simulating oceanic $CaCO_3$ export production in the greenhouse, Geophys. Res. Lett., 31, L16308, doi:10.1029/2004GL020613, 2004.

Intergovernmental Panel on Climatic Change (IPCC) , Third Assessment Report of Working Group III, Mitigation, edited by: Metz, B., Davidson, O., Swart, R., and Jiahua, P., 752 pp., Cambridge Univ. Press, New York, 2001.

Ito, T., and Deutsch, C.: Understanding the saturation state of argon in the thermocline: The role of air-sea gas exchange and diapycnal mixing, Global Biogeoche. Cy., 20, GB3019, doi:10.1029/2005GB002655, 2006.

Joos, F., Bruno, M., Fink, R. Stocker, T. F., Siegenthaler, U., Le Quéré, C., and Sarmiento, J. L.: An efficient and accurate representation of complex oceanic and biospheric models of anthropogenic carbon uptake, Tellus, 48B, 397–417, 1996.

Joos, F. and Bruno, M.: Pulse response functions are cost-efficient tools to model the link between carbon emissions, atmospheric CO_2 and global warming, Phys. Chem. Earth, 21, 471–476, 1996.

Joos, F., Plattner, G.-K., Stocker, T. F., Marchal, O., and Schmittner, A.: Global warming and marine carbon cycle feedbacks on future atmospheric CO_2, Science, 284, 464–467, 1999.

Joos, F., Prentice, I. C., Sitch, S., Meyer, R., Hooss, G., Plattner, G.-K., Gerber, S., and Hasselmann, K.: Global warming feedbacks on terrestrial carbon uptake under the Intergovernmental Panel on Climate Change (IPCC) emission scenarios, Global Biogeochem. Cy., 15, 891–908, 2001.

Key, R. M., Kozyr, A., Sabine, C. L., et al.: A global ocean carbon climatology: Results from Global Data Analysis Project (GLODAP), Global Biogeochem. Cy., 18, GB4031, doi:10.1029/2004GB002247, 2004.

Kraus, E. and Turner, J.: A one-dimensional model of the seasonal thermocline: II, Tellus, 19, 98–105, 1967.

Lenton, T. M. and Britton, C.: Enhanced carbonate and silicate weathering accelerates recovery from fossil fuel CO_2 perturbations, Global Biogeochem. Cy., 20, GB3009, doi:10.1029/2005GB002678, 2006.

Maier-Reimer, E. and Hasselmann, K.: Transport and storage of CO_2 in the ocean – an inorganic ocean – circulation carbon cycle model, Clim. Dynam., 2, 63–90, 1987.

Maier-Reimer, E.: Geochemical cycles in an ocean general circulation model: preindustrial tracer distributions, Global Biogeoche. Cy., 7, 645–677, 1993.

Maier-Reimer, E.: The biological pump in the greenhouse, Glob. Planet. Change, 8, 13–15, 1993.

Maier-Reimer, E., Mikolajewicz, U., and Winguth, A.: Future ocean uptake of CO_2: interaction between ocean circulation and biology, Clim. Dynam., 12, 711–721, 1996.

Marchal, O., Stocker, T. F., and Joos, F.: A latitude-depth, circulation-biogeochemical ocean model for paleoclimate studies: Model development and sensitivities, Tellus, 50B, 290–316, 1998.

Matsumoto, K., Sarmiento, J. L., Key, R. M., et al.: Evaluation of ocean carbon cycle models with data-based metrics, Geophys. Res. Lett., 31, L07303, doi:10.1029/2003GL018970, 2004.

Matsumoto, K., Tokos, S., Price, A., and Cox, S. J.: First description of the Minnesota Earth System Model for Ocean biogeo-

chemistry (MESMO 1.0), Geoscientific Model Development, 1, 1–15, 2008.

Meissner, K. J., Weaver, A. J., Matthews, H. D., and Cox, P. M.: The role of land-surface dynamics in glacial inception: a study with the UVic Earth System Model, Clim. Dynam., 21, 515–537, doi:10.1007/s00382-0352-2, 2003.

Mikolajewicz, U., Groger, M., Maier-Reimer, E., Schurgers, G., Vizcaino, M., and Winguth, A.: Long-term effects of anthropogenic CO_2 emissions simulated with a complex earth system model, Clim. Dynam., 28, 599–631, 2007.

Montenegro, A., Brovkin, V., Eby M., Archer, D., and Weaver A. J.: Long term fate of anthropogenic carbon, Geophys. Res. Lett., 34, L19707, doi:10.1029/2007GL030905, 2007.

Mouchet, A. and Francois, L.: Sensitivity of a global ocean carbon cycle model to the circulation and to the fate of organic matter: preliminary results, Phys. Chem. Earth., 21, 511–516, 1996.

Müller, S. A, Joos, F., Edwards, N. R., and Stocker, T. F.: Water mass distribution and ventilation time scales in a cost-efficient, three-dimensional ocean model, J. Climate, 19(21), 5479–5499, doi:10.1175/JCLI3911.1, 2006.

Murnane, R. J., Sarmiento, J. L., and Le Quéré, C.: Spatial distribution of air-sea CO_2 fluxes and the interhemispheric transport of carbon by the oceans, Global Biogeochem. Cy., 13, 287–305, 1999.

Najjar, R. G., Jin, X., Louanchi, F., et al.: Impact of circulation on export production, dissolved organic matter, and dissolved oxygen in the ocean: Results from Phase II of the Ocean Carbon-cycle Model Intercomparison Project (OCMIP-2), Global Biogeochem. Cy., 21, GB3007, doi:10.1029/2006GB002857, 2007.

Orr, J. C., Maier-Reimer, E., Mikolajewicz, U., et al.: Estimates of anthropogenic carbon uptake from four threedimensional global ocean models, Global Biogeochem. Cy., 15, 43–60, 2001.

Orr, J. C.: Global ocean storage of anthropogenic carbon, 116pp, Inst. Peirre Simon Laplace, Gid-sur-Yvette, France, 2002.

Orr, J. C., Fabry V., Aumont, O., et al.: Anthropogenic ocean acidification over the twenty first century and its impact on calcifying organisms, Nature, 437, 681–686, 2005.

Parekh, P., Joos F., and Müller, S. A.: A modeling assessment of the interplay between aeolian iron fluxes and ligands in controlling carbon dioxide fluctuations during Antarctic warm events, Paleoceanography, 23, PA4202, doi:10.1029/2007PA001531, 2008.

Plattner, G.- K., Joos, F., Stocker, T. F., and Marchal O.: Feedback mechanisms and sensitivities of ocean carbon uptake under global warming, Tellus, 53B, 564–592, 2001.

Plattner, G.-K., Knutti, R., Joos, F., et al.: Long-term climate commitments projected with climate – carbon cycle models, J. Climate, 21, 2721–2751, 2008.

Ridgwell, A., Hargreaves, J. C., Edwards, N. R., Annan, J. D., Lenton, T. M., Marsh, R., Yool, A., and Watson, A.: Marine geochemical data assimilation in an efficient Earth System Model of global biogeochemical cycling, Biogeosciences, 4, 87–104, 2007a,
http://www.biogeosciences.net/4/87/2007/.

Ridgwell, A., Zondervan, I., Hargreaves, J. C., Bijma, J., and Lenton, T. M.: Assessing the potential long-term increase of oceanic fossil fuel CO_2 uptake due to CO_2-calcification feedback, Biogeosciences, 4, 481–492, 2007b,
http://www.biogeosciences.net/4/481/2007/.

Ridgwell, A. and Hargreaves J. C.: Regulation of atmospheric CO_2 by deep-sea sediments in an Earth system model, Global Biogeochem. Cy., 21, GB2008, doi:10.1029/2006GB002764, 2007.

Roeckner, E., Arpe, K., Bengtsson, L., et al.: Simulation of the present-day climate with the ECHAM model: impact of the model physics and resolution, Report No. 93., Hamburg, 1992.

Royal Society: Ocean acidification due to increasing atmospheric carbon dioxide, The Royal society, London, 2005.

Sabine, C. L., Feely, R. A., Gruber, N., et al.: The Oceanic Sink for Atmospheric Carbon, Science, 305, 367–371, 2004.

Sarmiento, J. L., Orr, J. C., and Siegenthaler, U.: A perturbation simulation of CO_2 uptake in an ocean general circulation model, J. Geophys. Res., 97, 3621–3645, 1992.

Sarmiento, J. L., Hughes, T. M. C., Stouffer, R. J., and Manabe, S.: Simulated response of the ocean to anthropogenic climate warming, Nature, 393, 245–249, 1998.

Schlitzer, R.: An adjoint model for the determination of the mean oceanic circulation, air-sea fluxes and mixing coefficients, Ber. zur Polarforschung 156, Alfred-Wegener-Institut, Bremerhaven, 1995.

Schlitzer, R.: Carbon export in the Southern Ocean: Results from inverse modeling and comparison with satellite-based estimates, Deep Sea Res., Part II, 49, 1623–1644, 2002.

Schmittner, A., Oschlies, A., Giraud, X., Eby, M., and Simmons, H. L.: A global model of the marine ecosystem for long-term simulations: Sensitivity to ocean mixing, buoyancy forcing, particle sinking, and dissolved organic matter cycling, Global Biogeochem. Cy., 19, GB3004, doi:10.1029/2004GB002283, 2005.

Schmittner A., Oschlies, A., Matthews, H. D., and Galbraith, E. D.: Future changes in climate, ocean circulation, ecosystems and biogeochemical cycling simulated for a business-as-usual CO_2 emission scenario until year 4000 AD, Global Biogeochem. Cy., 22, GB1013, doi:10.1029/2007GB00295, 2008.

Shaffer, G. and Sarmiento, J. L.: Biogeochemical Cycling in the Global Ocean .1. A New, Analytical Model with Continuous Vertical Resolution and High-Latitude Dynamics, J Geophy. Res., 100, 2659–72, 1995.

Siegenthaler, U. and Oeschger, H.: Biospheric CO_2 emissions during the past 200 years reconstructed by deconvolution of ice core data, Tellus, 39B, 140–154, 1987.

Siegenthaler, U. and Joos, F.: Use of a simple model for studying oceanic tracer distributions and the global carbon cycle, Tellus, 44B, 186–207, 1992.

Singarayer, J. S., Richards, D. A., Ridgwell, A., Valdes, P. J., Austin, W. E. N., and Beck, J. W.: An oceanic origin for the increase of atmospheric radiocarbon during the Younger Dryas, Geophys. Res. Lett., 35, L14707, doi:10.1029/2008GL034074, 2008.

Steinacher, M., Joos, F., Frölicher, T. L., Plattner, G.-K., and Doney, S. C.: Imminent ocean acidification projected with the NCAR global coupled carbon cycle-climate model, Biogeosciences Discuss., 5, 4353–4393, 2008,
http://www.biogeosciences-discuss.net/5/4353/2008/.

Stocker, T. F., Wright, D. G., and Mysak, L. A.: A zonally averaged, coupled ocean-atmosphere model for paleoclimate studies, J. Climate, 5, 773–797, 1992.

Tschumi, T., Joos, F., and Parekh, P.: How important are Southern Hemisphere wind changes for low glacial carbon dioxide? A model study, Paleoceanography, 23, PA4208, doi:10.1029/2008PA001592, 2008.

Walker, J. C. G. and Kasting, J. F.: Effects of fuel and forest conservation on future levels of atmospheric carbon dioxide, Palaeogeog, Palaeoclimatol., Palaeoecol., 97, 151–189, 1992.

Waugh, D. W., Hall, T. M., Mcneil, B. I., Key, R., and Matear, R. J.: Anthropogenic CO_2 in the oceans estimated using transient time distributions, Tellus, 58B, 376–389, 2006.

Weaver, A. J., Eby, M., Wiebe, E. C., et al.: The UVic Earth System Climate Model: Model description, climatology and application to past, present and future climates, Atmos-Ocean, 38, 271–301, 2001.

Willey, D. A., Fine, R. A., Sonnerup, R. E., Bullister, J. L., Smethie Jr., W. M., and Warner, M. J.: Global oceanic chlorofluorocarbon inventory, Geophys. Res. Lett., 31, L01303, doi:10.1029/2003GL018816, 2004.

Winguth A., Heimann, M., Kurz, K. D., Maier-Reimer, E., Michajewicz, U., and Segschneider, J.: ENSO related fluctuations of the marine carbon cycle, Global Biogeochem. Cy., 8, 39–65, 1994.

Wright, D. G. and Stocker, T. F.: Sensitivities of a zonally averaged global ocean circulation model, J. Geophys. Res., 97, 12707–12730, 1992.

Wright, D. G. and Stocker, T. F.: Closures used in zonally averaged ocean models, J. Phys. Oceanogr., 28, 701–804, 1998.

Yamanaka, Y. and Tajika E.: The role of the vertical fluxes of particulate organic matter and calcite in the oceanic carbon cycle: Studies using an ocean biogeochemical circulation model, Global Biogeochem. Cy., 10, 361–382, 1996.

Zeebe, R. E. and Caldeira K.: Close mass balance of long-term carbon fluxes from ice-core CO_2 and ocean chemistry records, Nature Geoscience, 1, 312–315, doi:10.1038/ngeo185, 2008.

Zickfeld, K., Fyfe, J. C., Saenko, O. A., Eby, M., and Weaver, A. J.: Response of the global carbon cycle to human-induced changes in Southern Hemisphere winds, Geophys. Res. Lett., 34, L12712, doi:10.1029/2006GL028797, 2007.